J Therm Anal Calorim (2012) 108:95–100
DOI 10.1007/s10973-011-1569-7

AMP.PNP affects the dynamical properties of monomer and polymerized actin

A DSC and an EPR study

K. Türmer · F. Könczöl · D. Lőrinczy · J. Belágyi

Received: 12 March 2011 / Accepted: 5 April 2011 / Published online: 1 May 2011

Abstract Actin is the component of several biological systems and it plays important role in different biological processes, especially in cell motility. The actin-based motility is accompanied with ATP-consume, and the irreversible ATP hydrolysis is coupled with the polymerization of monomer actin into filamentous form. When an actin monomer is incorporated into a filament, the ATPase is activated, and thereby the polymer formation is promoted. The polymer formation and the ATP hydrolysis is associated with internal motions and significant changes of the conformation in reaction partners. In this article, the ATP nucleotide in monomer actin was exchanged by its non-hydrolyzable analogue adenylyl-imidodiphosphate (AMP.PNP), and using two biophysical methods, electron paramagnetic resonance spectroscopy (EPR) and differential scanning calorimetry (DSC), we studied the local and global changes in globular and fibrous actin following the nucleotide exchange. The paramagnetic probe molecule—a maleimide spin label—was attached to Cys-374 site of monomer actin, and its rotational mobility was derived at different temperature. In DSC measurements the transition temperatures of samples with different bound nucleotides were compared. From the measurements we could conclude, that the nucleotide exchange induces changes in the internal rigidity of the actin systems, AMP.PNP-actins showed longer rotational correlation time and increased thermal transition temperature.

K. Türmer · D. Lőrinczy (✉) · J. Belágyi
Faculty of Medicine, Institute of Biophysics, University of Pécs, 7624 PécsSzigeti str. 12, Hungary
e-mail: denes.lorinczy@aok.pte.hu

F. Könczöl
Faculty of Medicine, Institute of Forensic Medicine, University of Pécs, 7624 PécsSzigeti str. 12, Hungary

Keywords ATP-G-actin · AMP.PNP-G-actin · Nucleotide exchange · Conformations of actins

Introduction

Actin is one of the main components in eukaryote cells which plays significant role in many cellular processes, like force-generation, maintenance of the shape of cells, cell-division cycle, and transport processes. Many structural investigations showed that the monomer actin (G-actin) consists of four subdomains, the internal structure of subdomains are stabilized by nucleotide, either ATP or ADP and a divalent cation (calcium or magnesium). The structure of subdomains is dynamic, as derived by several biophysical and structural studies; the subdomain might have different motional states depending on the bound cations and nucleotides [1–3]. Site-specific cross-linking among F-actin monomers inhibits the motion and force generation in myosin [4, 5]. The ability of G-actin to reversible polymerize into long filaments is essential for many cellular functions.

The structure of monomer and polymerized actins, ATP- and ADP-actins were mainly obtained from crystal structures of actin and derived from interactions with different proteins. The detailed investigations concluded that ATP-actin monomers and ADP-actin monomers were structurally different, and they exhibited nucleotide-dependent internal motion in polymerized form [6–8]. Similarly, structural differences were observed in the nature of the tightly bound divalent cations Ca^{2+} and Mg^{2+} [9]. The nucleotides and the cations are located in the cleft in the center of the molecule. The cleft might be in open or closed conformation, in which the two larger domains are twisted relative to each other. The opening of cleft affects the

binding mode of nucleotides, and might be in relation with the nucleotide release [7]. The exchange of the nucleotide and/or the cations affects the structure of subdomain 2 and the C terminal region of actin [3, 9–11].

The different functions of actin require special internal organization in time and space, and special interactions with other molecules at well-defined regions [1, 3]. Two basic techniques, such as DSC and EPR, were applied in the present article to study how the bound nucleotides affect the local dynamics of actin. A site-directed paramagnetic reporter molecule—a maleimide spin label—was already successfully attached to Cys-374 amino acid residue in many scientific reports, which allowed to map the cation-induced motional changes, and to study how these motional states vary at different temperatures [12–14]. By an approximation of the Lumry–Eyring model the thermal transitions of monomer actin were analyzed, and by deconvolution of the DSC transitions it was possible to study the interactions between larger subdomains affected by divalent cations [15].

Recently, precise structural experiments showed that the symmetry and the parameters of crystals of AMP.PNP-actin are identical with the ADP-actin structure [6]. However, the release of nucleotide γ-phosphate induces conformational change, which might induce increase or decrease of internal motions. The reporter molecules which are located in the groove of subdomain 1 might report changes in the hydrophobic pocket near the COOH-terminus. Removal of calcium or ATP resulted in significant change of rotational correlation times in both populations. Substituting ATP with its non-hydrolysable ATP analog adenylyl-imidodiphosphate (AMP.PNP) also affected the internal motions in monomer actin, as well as in its polymerized form AMP.PNP-F-actin. Analysis of DSC transitions in the presence of AMP.PNP-G-actin and AMP.PNP-F-actin showed that the local internal motions detected by EPR measurements are coupled with global motions and conformational changes measured by DSC.

Materials and methods

Protein purification and modification

Actin was purified from the domestic white rabbit skeletal back and leg muscles. The actin was stored in buffer A (0.2 mM ATP, 0.1 mM $CaCl_2$, 4 mM MOPS, pH 8). G-actin concentration was determined by absorbance at 290 nm using a molar extinction coefficient of 0.63 mg^{-1} $mlcm^{-1}$ using a Shimadzu UV 2100 spectrophotometer. F-actin was prepared by the addition of 2 mM $MgCl_2$ and 100 mM KCl to buffer A.

Spin labeling of actin

Actin was spin-labeled with *N*-(1-oxyl-2,2,6,6,-tetramethyl-4-piperidinyl)-maleimide spin label (MSL) in F-form in a molar ratio of 1:1.2 for 12 h at 4 °C. Unreacted labels were removed by pelleting the actin by ultracentrifugation. The pellet was resuspended, homogenized and dialyzed in buffer A.

Preparation of nucleotide-free actin

Nucleotide-free actin was prepared by mixing actin with Dowex 1(Dowex 1:distilled water 1:1). 150 µL Dowex 1 to 1 mL actin was used to remove nucleotides, incubating the sample at room temperature for 5 min. Dowex 1 was removed by centrifugation on 4 °C at 13,000 rpm for 3 min, and actin was collected from the pelleted Dowex 1. This procedure was repeated to dissociate the bound ATP. The treatment removes about 80% of the bound nucleotide [16].

Binding of AMP.PNP to actin

Excess ATP was removed from actin, and proportional amounts of AMP.PNP were then added to the actin.

EPR spectroscopy

Conventional and ST EPR spectra of actin were recorded with an ESP 300E X-band spectrometer (Bruker Biospin, Rheinstetten, Germany). First harmonic in-phase, absorption spectra were obtained using 20 mW microwave power and 100 kHz field modulation with amplitude of 0.15 mT. Actin concentration varied between 30 and 120 µM; the spectra were recorded at ambient temperature. The protein samples were placed in two capillary tubes (Mettler ME-18552 melting point tubes), each of them contained 10 µL solution. The sample tubes were positioned parallel in the centre region of the TM 110 cylindrical cavity. A small thermocouple was inserted in one of the capillary tubes, and the temperature was regulated with a diTC2007 type temperature controller. Studying the EPR spectra of actin as a function of temperature, the temperature was varied between 0 and 60 °C with an accuracy of 0.5 °C. Saturation transfer EPR spectra were measured as described in [17].

DSC measurement

Thermal unfolding of actin was monitored by SETARAM Micro DSC III calorimeter. All experiments were performed between 20 and 100 °C, the heating rate was 0.3°K/min in all cases. We used conventional Hastelloy batch

vessels for the experiments with 800 μL sample volume. The sample and reference vessels were equilibrated with a precision of 0.1 mg. Buffer A solutions (0.2 mM ATP, 0.1 mM $CaCl_2$, 4 mM MOPS, pH 8 or the same buffer A without ATP) were used as a reference sample. The repeated scan of denatured sample was used as baseline reference, which was subtracted from the original DSC curve. Simple mathematical calculations were used to obtain the thermodynamic data of samples (excess heat capacity $C_{p,ex}$, transition temperature T_m and calorimetric enthalpy change ΔH).

Computational methods

The EPR spectra was evaluated with the WINEPR program from Bruker and with a computer program developed in our laboratory. The experimental thermograms were compared with the simulated ones using the calculated excess heat capacities according to the procedure from Sanchez-Ruiz [18] and Conjero-Lara et al. [19]. The simulated heat transition curves approximate well the measured transitions.

Results and discussion

Actin isolated from skeletal muscle of rabbit was spin-labeled in F-form with maleimide nitroxide (MSL). In G-form of actin the labels were strongly immobilized on the Cys-374 amino acid residues, and rotated with an effective rotational correlation time in the nanosecond time domain (~18 ns, Fig. 1). However, one part of the probe molecules (about 10% or smaller) according their apparent mobility were bound either at different sites, or which is more probable that the reporter molecules were located on the same sites; but the distribution of these attached labels exhibits some non-uniformity, which appears as a smaller rotational correlation time in the range of a few nanoseconds (3–4 ns). The amount of this fraction depends critically on temperature. In F-form of actin the immobilizing effect on the probe molecules is significantly larger as can be measured by the ST EPR technique ($\tau_2 \sim$ 100–150 μs for MSL-F-actin), and the contribution of the more mobile fraction is significantly reduced [12, 17].

Increase of temperature of the samples in the microwave cavity induced a continuous decrease of the hyperfine splitting constant $2A'_{zz}$, which is the result of the increased rotational mobility of the labels and a rapid increase of the ratio of the two peaks characterizing the weakly and strongly immobilized components (Fig. 1). Over 60 °C only the weakly immobilized components could be detected. This temperature is already coincides with the denaturation temperature of the monomer actin. The temperature dependence of $2A'_{zz}$ against reciprocal absolute

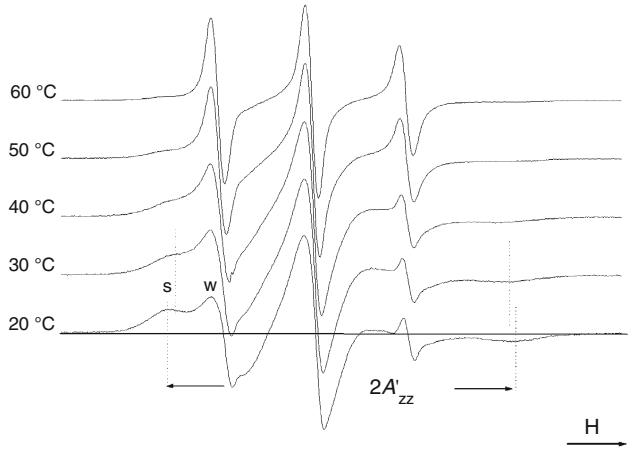

Fig. 1 EPR spectra of MSL-ATP-G-actin at different temperature. At increasing temperature the hyperfine splitting constant ($2A'_{zz}$) decreases, the intensity ratio of the first two peaks (w/s) increases

temperature (1,000/T) in the case of nucleotide-free G-actin and nucleotide-free F-actin exhibited only a small decrease of $2A'_{zz}$ in comparison with ATP-G-actin and ADP-F-actin (data for F-actin are not shown in Fig. 2). It is known from earlier articles that the removal of nucleotides produces the rapid and irreversible denaturation of G-actin, but the structure of nucleotide-free F-actin filament system did not show large difference from ADP-F-actin [20]. From the 2.5 nm resolution of the three-dimensional reconstruction similar intersubunit contacts were derived. Therefore, a significant mobility increase cannot be expected in the environment of the probe molecules. It was also concluded that ATP is not required for assembly of stable filaments. The larger, but not significant slope for nucleotide-free G-actin supports the former conclusion that the environment of paramagnetic probe molecule does not sensitive to the presence or absence of the nucleotide in the hydrophobic region between the 1 and 3 domains. In contrast, removing Ca-ions from the MSL-G-actin by EGTA produced an increase of the hyperfine splitting value, which is the sign of the slow polymerization of monomer actin. Simultaneously, a marked increase of mobility appeared in the environment of the Cys-374 residue. In the presence of Mg-ions the immobilization of the MSL-label is more pronounced.

Manipulation with the bound nucleotide on Ca-G-actin with AMP.PNP did not induce a marked change in the distribution of the two fractions of the bound labels, but the environment of the immobile fraction of labels showed an increasing immobilization in comparison to ATP-G-actin (Fig. 2). ATP is tightly bound to subdomains 3 and 4. A possible explanation for increased immobilization might be that the substitution of the nucleotides produces a small relative rotation of the two domains which leads to a structural immobilization for AMP.PNP-G-actin.

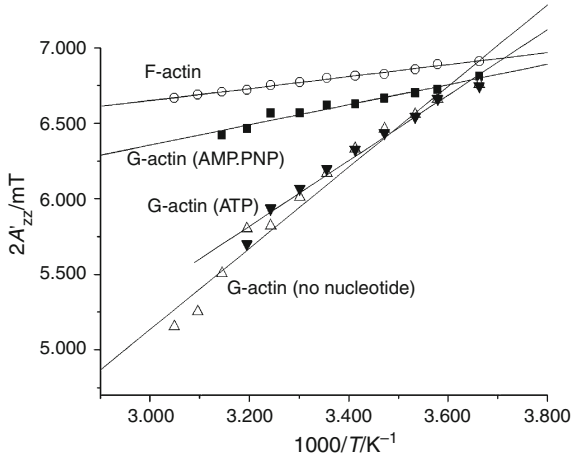

Fig. 2 Temperature dependence of $2A'_{zz}$ against reciprocal absolute temperature at different preparations. The slopes report the average change in mobility. Significantly smaller slop of AMP.PNP-G-actin in comparison to ATP-G-actin refers to the increased internal rigidity of the monomers after nucleotide exchange. In contrast the difference between slopes for ATP-G-actin and nucleotide-free G-actin can be neglected. Similarly, little difference was found between ADP-F-actin and AMP.PNP-F-actin (data are not shown)

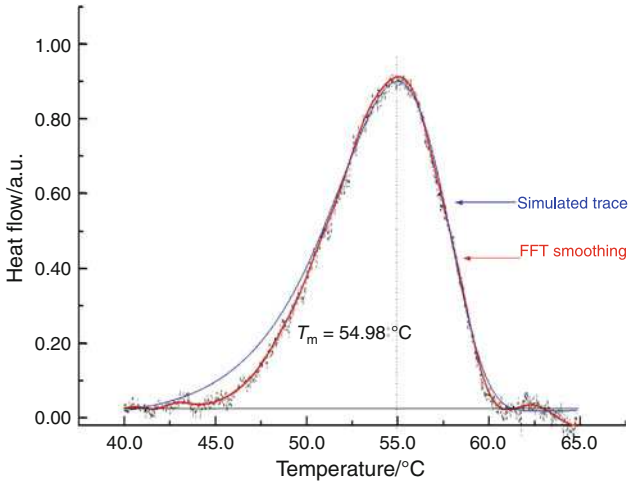

Fig. 3 DSC trace of ATP-G-actin. The concentration of G-actin was 69.0 μM, the *blue line* shows the simulated heat transition

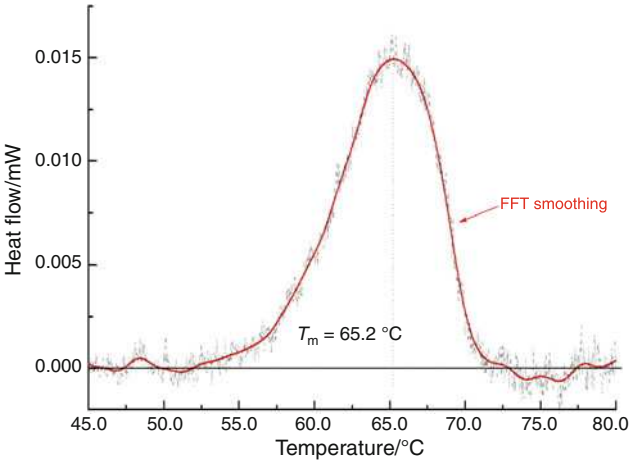

Fig. 4 DSC transition of AMP.PNP-G-actin. The transition temperature is significantly higher than in the case of ATP-G-actin. The concentration of actin sample was 70 μM

The DSC transitions of G- and F-actin were calorimetrically irreversible. Lumry and Eyring [15] and Sanchez-Ruiz [18] in their basic reports suggested that, in many cases, the irreversible denaturation of proteins by DSC can be described on the basis of a simple two-state irreversible model [15–19]:

$$N \xrightarrow{k_{ap}} F$$

The k_{ap} reaction rate constant that governs the conversion from native to folded state is strongly temperature-dependent, and is a first-order rate constant. Following the suggested procedure, the analysis of DSC transitions showed that the local internal motions and conformational changes—detected by EPR measurements—are coupled with global motions and phase transitions measured by DSC. Figure 3 shows the thermal transition of G-actin with bound nucleotide ATP. The transition temperature was (55.6 ± 1.5) °C ($n = 3$). In the case of untreated ADP-F-actin the transition temperature increased up to about (67.1 ± 0.8 °C SEM, $n = 5$), which is due to the polymer formation and to the increased cooperative interaction between the monomers (Fig. 4). These values agree quite well with data published on earlier measurements [10, 21, 22].

DSC measurements on AMP.PNP-G-actin and AMP.PNP-F-actin resulted in significant increase of the thermal transition temperature, for monomer actin (65.3 ± 0.5 °C SEM, $n = 7$) was obtained, whereas (72.6 ± 1.0 °C SEM, $n = 6$) temperature was calculated. The results are in correlation with the EPR measurements, that is, the substitution of ATP or ADP with the non-hydrolyzable ATP analogue accompanied with significant heat stabilization.

The experimental thermograms were compared with the simulated ones using the calculated excess heat capacities according to the procedure from Conjero-Lara et al. [19]. The simulated heat transition curves approximate quite well the measured transitions (see Figs. 3 and 4). The small deviation between the measured and simulated curves can be explained by the fact that in most cases by FFT smoothened transition curves were used at the evaluation of the thermodynamic parameters because of the unfavorable signal to noise ratio of the original DSC trace (Figs. 5, 6).

In summary, the mobility and thermodynamic differences obtained in these experiments by the two methods after substitution of ATP with the non-hydrolyzable ATP

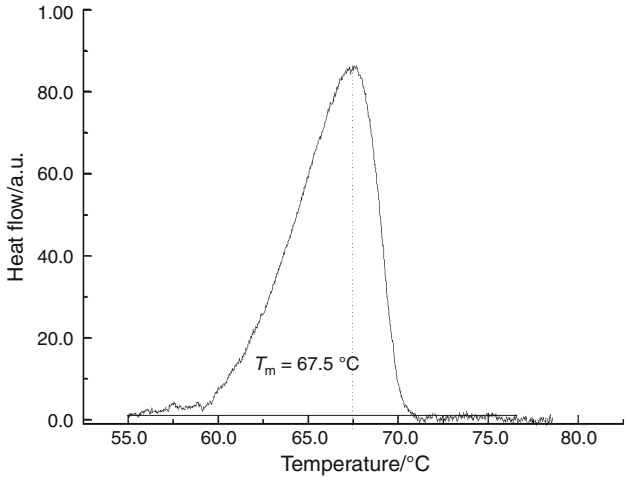

Fig. 5 DSC trace of ADP-F-actin. The concentration of sample was 170 μM

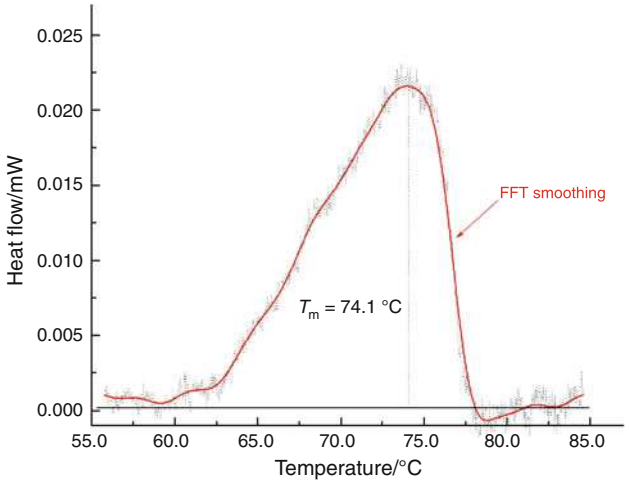

Fig. 6 DSC transition of AMP.PNP-F-actin. The concentration of actin sample was 50 μM. The significantly larger transition temperature refers to the increased rigidity

analogue provide a simple model how to interpret the result of the hydrolysis of ATP during the formation of actin polymer. The EPR and DSC measurements as well showed on ATP-G-actin and AMP.PNP-G-actin that the nucleotide exchange leads to a decreased internal flexibility. The ATP hydrolysis may change the conformations of the actin monomers during filament formation which might contribute to the change of flexibility of the actin filaments [23]. In F-form of actins only a small change was detected on AMP.PMP-F-actin in comparison with ADP-F-actin. The flexibility of filaments is essential for the proper function of F-actin in biological systems.

References

1. Egelman EH, Orlova A. New insights into actin filament dynamics. Curr Opin Struct Biol. 1995;5:172–80.
2. Orlova A, Egelman EH. A conformational change in the actin the subunit can change the flexibility of the actin filament. J Mol Biol. 1993;232:334–41.
3. Orlova A, Egelman EH. Structural dynamics of F-actin. I. Changes in the C-terminus. J Mol Biol. 1995;245:582–97.
4. Kim E, Bobkova E, Miller CJ, Orlova A, Hegyi G, Egelman EH, Muhlrad A, Reisler E. Intrastrand cross-linked actin between Gln41 and Cys374. III. Inhibition of motion and force generation with myosin. Biochemistry. 1998;37:17801–9.
5. Könczöl F, Lőrinczy D, Vértes Zs, Hegyi G, Belágyi J. Intermonomer cross-linking affects the thermal transitions in F-actin. J Therm Anal Calorim. 2010;101:549–53.
6. Otterbein LR, Graceffa P, Domingez R. The crystal structure of uncomplexed actin in the ADP state. Science. 2001;293:708–11.
7. Graceffa P, Domingez R. Crystal structure of monomeric actin in the ATP state. J Biol Chem. 2003;278:34172–80.
8. Gaszner B, Nyitrai M, Hartvig N, Köszegi T, Somogyi B, Belagyi J. Replacement of ATP with ADP affects the dynamic and conformational properties of actin monomer. Biochemistry. 1999;38:12885–92.
9. Strzelecka-Golaszewska H, Moraczewska J, Khaitlina SY, Mossakowska M. Localization of the tightly bound divalent-cation-dependent and nucleotide-dependent conformation changes in G-actin using limited proteolytic digestion. Eur J Biochem. 1993;311:731–42.
10. Levitsky D, Pivovarova AV, Mikhailova VV, Nikolaeva OP. Thermal unfolding and aggregation of actin. Stabilization and destabilization of actin filaments. FEBS J. 2008;275:4280–95.
11. Nikolaeva OP, Dedova IV, Khvorova IS, Levitsky DI. Interaction of F-actin with phosphate analogues studied by differential scanning calorimetry. FEBS Lett. 1994;351:15–8.
12. Thomas DD, Seidel JC, Gergely J. Rotational dynamics of spin-labeled F-actin in the sub-millisecond time range. J Mol Biol. 1979;132:257–73.
13. Yoshimura HT, Nishio K, Mihashi K, Kinosita Jr, Ikegami K. Torsional motion of eosin-labeled F-actin as detected in the time-resolved anisotropy decay of the probe in the sub-millisecond time range. J Mol Biol. 1984;179:453–67.
14. Prochniewicz E, Zhang Q, Howard EC, Thomas DD. Microsecond rotational dynamics of actin: spectroscopic detection and theoretical simulation. J Mol Biol. 1996;255:446–57.
15. Lumry R, Eyring J. Conformation changes in proteins. J Phys Chem. 1954;58:110–34.
16. De La Cruz EM, Pollard TD. Nucleotide-free actin: stabilization by sucrose and nucleotide binding kinetics. Biochemistry. 1995;34:5452–61.
17. Kupi T, Gróf P, Nyitrai M, Belagyi J. The uncoupling of the effects of formins on the local and global dynamics of actin filaments. Biophys J. 2009;96:474–88.
18. Sanchez-Ruiz JM. Theoretical analysis of Lumry-Eyring models in differential scanning calorimetry. Biophys J. 1992;61:921–35.
19. Conjero-Lara F, Mateo PL, Aviles FX, Sanchez-Ruiz JM. Effect of Zn^{++} on the thermal denaturation of carboxypeptiase B. Biochemistry. 1991;30:2067–72.
20. De La Cruz EM, Mandinova A, Steinmetz MO, Stoffler D, Aebi U, Pollard TD. Polymerization and structure of nucleotide-free actin filaments. J Mol Biol. 2000;295:516–7.
21. Bertazzon A, Tian GH, Lamblin A, Tsong TY. Enthalpic and enthropic contributions to actin stability: calorimetry, circular

dichroism, and fluorescence study and effects of calcium. Biochemistry. 1990;29:291–8.
22. Lőrinczy D, Vértes Zs, Könczöl F, Belagyi J. Thermal transitions of actin. J Therm Anal Calorim. 2009;100:713–79.
23. Oda T, Iwasa M, Aihara T, Maeda Y, Narita A. The nature of the globular-to fibrous-actin transition. Nature. 2009;457:441–5.